Neuroprotective effects of CysLT2R antagonist on Angiostrongylus cantonensis-induced edema and meningoencephalitis

Ke-Min Chen
Chung Shan Medical University
Shih-Chan Lai
shih@csmu.edu.tw

Chung Shan Medical University

Research Article

Keywords: Angiostrongylus cantonensis, CysLT2R, edema, HAMI3379, meningoencephalitis

Posted Date: October 28th, 2023

DOI: https://doi.org/10.21203/rs.3.rs-3483627/v1

Additional Declarations: No competing interests reported.

Version of Record: A version of this preprint was published at Molecular and Biochemical Parasitology on July 1st, 2024. See the published version at https://doi.org/10.1016/j.molbiopara.2024.111649.

Abstract

Background

The pathogenesis of *Angiostrongylus cantonensis*-induced eosinophilic meningoencephalitis includes haemorrhage, brain edema formation, disrupting the blood–brain barrier (BBB), and induction of an inflammatory response. Cysteinyl leukotrienes (CysLTs) can induce a disruption of the BBB, and this reaction is mediated by cysteinyl-leukotriene receptors. In this study, we used *A. cantonensis*-induced eosinophilic meningoencephalitis as a model to investigate whether the CysLT2 receptor involved in the pathogenesis of angiostrongyliasis meningoencephalitis.

Methods

The brain edema was determined using the wet weight/dry weight method. Microglia polarization was detected by Flow cytometry and Enzyme-linked immunosorbent assay. Evans blue method was used to measure changes in the blood brain barrier, while western blotting was used to analyze BBB-related proteins. Gelatin zymography was used to assay matrix metalloproteinase-9 (MMP-9). MicroRNA expression was detected by Quantitative reverse transcription-PCR (qRT-PCR).

Results

The present study provides evidence that the CysLT2 receptor antagonist HAMI3379 reduced the number of infiltrated eosinophils and brain edema in eosinophilic meningoencephalitis. Additionally, we found that HAMI3379 significantly decreased the protein levels of M1 polarisation markers (CD80, iNOS, IL-5 and TNF-α), increased the expression of M2 polarisation markers (CD206, IL-10 and TGF-β) both *in vivo* and *in vitro*. Matrix metalloproteinase-9, S100B, GFAP, fibronectin, and claudin-5 were markedly lower after HAMI3379 treatment. Therefore, HAMI3379 reduced the BBB dysfunction in angiostrongyliasis meningoencephalitis. We have identified microRNA-155 as a BBB dysfunction marker in eosinophilic meningoencephalitis. The results showed that microRNA-155 was 15-fold upregulated in eosinophilic meningoencephalitis and 20-fold upregulated after HAMI3379 treatment.

Conclusions

Our results suggest that CysLT2R may be involved in *A. cantonensis*-induced brain edema and eosinophilic meningoencephalitis and that down-regulation of CysLT2R could be a novel and potential therapeutic strategy for the treatment of angiostrongyliasis meningoencephalitis.

Background

Rat lungworm *Angiostrongylus cantonensis* infection can cause eosinophilic meningoencephalitis and mechanical tissue injury to the brain [1]. The pathogenesis of eosinophilic meningoencephalitis includes haemorrhage, brain edema formation, disrupting the blood–brain barrier (BBB), and induction of an inflammatory response [2]. A critical event in the development of brain edema is the breakdown of the BBB, which can be initiated and regulated by several pro-inflammatory mediators including oxidative mediators, adhesion molecules, cytokines, and chemokines [3]. These mediators not only regulate the magnitude of leukocyte extravasation into the brain parenchyma, but also act directly on brain endothelial cells, causing loosening of junction complexes between endothelial cells, increasing the permeability of the brain endothelial barrier and causing vasogenic edema.

Neuroinflammation is induced when the neurovascular unit responds to specific stimuli involved in the activation of microglia, the breakdown of the BBB, the infiltration of peripheral leukocytes and inflammation factors [4]. The neurovascular unit is a complex multi-cellular structure consisting of endothelial cells, neurons, glia, smooth muscle cells, and pericytes [5]. As a crucial component of the neurovascular unit, microglia interact with the endothelium and modulate the BBB [6]. Microglia are activated in two polarisation states: the pro-inflammatory (M1) and anti-inflammatory (M2). Alterations in the M1/M2 polarisation phenotype can affect neuroinflammation progression, and inhibition of neuroinflammation corresponding to reduced microglia of M1 and increased M2 [7].

Cysteinyl leukotrienes (CysLTs) modulates CNS inflammatory diseases primarily through the CysLT1 receptor and the CysLT2 receptor; they can induce BBB disruption and brain edema [8]. The CysLT1 receptor regulates increased permeability of the BBB and related vasogenic brain edema, astrocyte proliferation, and inflammatory responses after brain ischemia [9]. However, the pathophysiological roles of CysLT2R are less known in the CNS diseases. It is not yet known whether the CysLT2 receptor antagonist HAMI3379 inhibits inflammatory responses such as microglial activation, eosinophil infiltration, or the generation of inflammatory cytokines. Thus, we sought to investigate the mechanisms of the CysLT2 receptor in *A. cantonensis*-induced brain edema and eosinophilic meningoencephalitis.

In the present study, we used *A. cantonensis*-induced eosinophilic meningoencephalitis as a model to investigate whether the CysLT2 receptor involved in the pathogenesis of angiostrongyliasis meningoencephalitis. The protection effects of the CysLT2R antagonist HAMI3379 on brain edema and meningoencephalitis were evaluated in a mouse model. The results provided a theoretical basis for further exploration of the possible inflammatory regulation mechanism of the CysLT2 receptor antagonist HAMI3379 in angiostrongyliasis meningoencephalitis.

Materials and Methods

Experimental animals

A total of 90 C57BL/6 strain male mice were purchased from the National Laboratory Animal Center, Taipei, Taiwan. All mice were kept in a 12 h light/dark cycle photoperiod and raised to 5 weeks old

(weighing 20–25 g). The mice received Purina Laboratory chow and water *ad libitum water.* The animals were kept in a specific pathogen-free room at the Animal Center, Chung-Shan Medical University (Taichung, Taiwan) for more than 1 week before the experimental infection [10]. The mice were inspected daily for the adequacy of food, water, bedding, and health conditions. After *A. cantonensis* infection, mice were monitored for signs of illness (ruffled fur, decreased activity or tachypnea) and weight loss. No mortality was observed in the mice during their infection and drug treatment. The mice were maintained under CO_2 flow for at least one minute after respiratory arrest. Cervical dislocation was performed as a confirmatory euthanasia method prior to necropsy. This study was carried out with the approval of the Institutional Animal Care and Use Committee of Chung-Shan Medical University and in accordance with the institutional guidelines for animal experiments.

Antibodies

Anti-mouse monoclonal antibodies for CD80 and CD206 were purchased from R&D Systems (USA). Polyclonal antibodies for goat anti-mouse arginase-1 (claudin-5, CysLT2R, fibronectin) were purchased from Santa Cruz Biotechnology (CA, USA). Goat anti-mouse caspase-1 (iNOS, GFAP, S100B) polyclonal antibodies were purchased from Cell Signaling Technology (Danvers, MA, USA). Anti-mouse β-actin monoclonal antibody was purchased from Sigma (St. Louis, MO, USA).

Larval preparation

The infective larvae (third stage, L3) of *A. cantonensis* were obtained from *Achatina fulica* snails, which were propagated for several months and infected with larvae of the first stage of *A. cantonensis* by rats at the Wufeng Experimental Farm (Taichung, Taiwan). The L3 larvae within the tissues were recovered using a method previously described but with several modifications [11]. The snail shells were crushed and tissues were homogenised in a pepsin-HCl solution (pH 1 to 2, 500 IU of pepsin / g of tissue) and digested by agitation at 37°C for 2 h. The L3 larvae in the sediment were collected by serial washes with double distilled water and counted under a microscope.

Treatment of animals

A total of 90 C57BL/6 male mice were randomly divided into six groups (15 mice/group). Food and water were withheld for 12 h before infection. Uninfected control mice were orally administered with distilled water for 10 consecutive days staring on day 10 post-inoculation (PI). All other groups were infected with 30 *A. cantonensis* larvae, including the infected untreated control mice that were orally treated with distilled water only on day 10 PI. Treatment mice were separately treated with DMSO alone (10 mg/kg/day, Sigma, USA), ABZ alone (10 mg/kg/day, Zentel®, GlaxoSmith Kline, NC, USA), HAMI 3379 alone (10 mg/kg/day, Cayman Chemical, USA) and ABZ–HAMI 3379 cotreatment (10 mg each/kg/day) for 7 consecutive days starting on day 10 PI. Mice were sacrificed 20 days after inoculation.

Preparation of excretory and secretory products (ESPs)

Third stage infectious *A. cantonensis* larvae were obtained from *Achatina fulica* as previously described [11] to infect mice, and young adult *A. cantonensis* were harvested from mouse brains 20 days after

infection, washed repeatedly to remove host cells. A total of 200 intracranial larvae were placed in 400 mL of sterile water. The worms were ground with a clear glass pestle, sonicated on ice (75 W for 10 seconds, 10 times, with 2-minute intervals) three times to release the soluble antigens. After centrifugation at 11,500g for 5 minutes at 4°C, the supernatant was recovered and filtered through a 0.22-mm filter. The total protein concentration in the filtrate was determined using the bicinchoninic acid method and the ESPs were stored at -80°C until further use.

Cell culture and stimulation assay

The mouse microglial cell line N9, which is derived from the American Type Culture Collection, was cultured in RPMI 1640 medium (Gibco, Carlsbad, CA, USA) containing 10% foetal bovine serum (Gibco, Carlsbad, CA, USA) and incubated at 37°C in a humidified atmosphere of 5% CO2. The cells were cultured in a 12-well culture plate (Corning, NY, USA) at a density of 1×10^5 cells per well. After formation of a monolayer, cells were stimulated with 50 μg/mL of ESPs as a positive control. The negative control group was added to an equal volume of liquid, which was extracted according to the ESPs preparation procedure without culturing *A. cantonensis*.

Treatment of microglia

For HAMI3379 treatment experiments, N9 microglial cells were cultured in 12-well plates (Corning) at a concentration of 1×10^5 cells per well. After formation of a monolayer, cells were stimulated with 50 μg/mL of ESPs and treated with 10 μM HAMI3379. Cells were collected 12 hours after ESPs stimulation and HAMI3379 treatment. The same vehicle concentration (DMSO) without HAMI3379 was administered to cells in vehicle control groups. Cells were harvested and lysed using mammalian cell lysis reagent (Fermentas, Hanover, MD, USA), and all cell homogenate samples were stored at -80°C until analysis.

CSF collection

Mice were anesthesized by intraperitoneal urethane (1.25g/kg) injection. Mice placed in a stationary instrument with 135 degree from the head and body. Skin of neck shaved and swabbed with 70% ethanol (three times). Subcutaneous tissue and muscles were separated. Capillary tube through dura mater into citerna magna and CSF well inpoured capillary tube. Inject CSF into a 0.5 ml eppendorf tube and centrifuged at 3000×*g* at 4°C for 5 min. Collection of supernatant in a 0.5 ml eppendorf tube and kept at -80°C freezer.

Eosinophil counts in the CSF

The CSF was collected in a centrifuge to rotate at 400×g for 10 min. Sediments were gently mixed with 100 μL Unopette buffer (Vacutainer System, Becton Dickinson, Franklin Lakes, NJ, USA) and 2 μL acetic acid and used a hemocytometer cell counting chamber (Paul Marienfeld, Lauda-Koenigshofen, Germany) was used to count eosinophils.

Evaluation of brain edema

The brain water content (brain edema) was determined using the wet weight/dry weight method as previously described [12]. Briefly, mice under 10% chloral hydrate (50 mg/kg) anaesthesia administered intraperitoneally were decapitated. Brain samples were quickly removed and divided into 3 parts: the ipsilateral hemisphere, the contralateral hemisphere, and the cerebellum. The cerebellum was used as an internal control of the water content. All samples were weighed on an electronic analytical balance (Sartorius BS 210 S; Sartorius UK Ltd., Epsom, UK) before and after drying (at 110 ° C for 24 h). The brain water content was calculated as [(wet weight − dry weight)/(wet weight)] × 100%.

Quantitative reverse transcription-PCR (qRT-PCR) assay

Total RNA was extracted and isolated from cultured cells and mice cerebrum tissue using the EZ2 RNA/miRNA Tissue/Cell Kit (QIAGEN) according to the manufacturer's instructions. The quantity of RNA samples was determined using NanoDrop One (Thermo Scientific).

For quantitative analysis of microRNA-155 expression, total RNA was reverse transcribed to cDNA using the TaqMan® MicroRNA Reverse Transcription Kit (Applied Biosystems, Foster City, CA, US) following the manufacturer’s instructions. Briefly, reverse transcription could be used in a reaction mixture containing 10 ng total RNA, 50 nM RT primer, 100 mM dNTPs, 50 U/ml MultiScribe reverse transcriptase, 20 U/μl RNase inhibitor, 10X reverse transcription buffer, and nuclease-free water. The RT reaction mixture will be incubated at 16℃ for 30 min, 42℃ for 30 min and then stopped at 85℃ for 5min. qRT-PCR was set up and run on the Applied Biosystems 7900HT real-time PCR System following the manufacturer's instructions. Briefly, qRT-PCR was performed using TaqMan Universal Master Mix II with UNG and TaqMan® MicroRNA Assays (Applied Biosystems) for the target microRNA. The reaction was carried out at 50°C for 2 min, 95°C for 10 min, followed by 40 amplification cycles at 95°C for 15 seconds and 60°C for 1 min. One nanogram of cDNA was used in each PCR reaction, and all samples were amplified simultaneously in triplicate in a single run. The expression levels were normalized to that of U6 small nuclear RNA and were calculated as fold differences ($2^{-\Delta\Delta Ct}$) from the normal control expression levels. The expression levels of U6 were not statistically different between all groups in this study.

For quantitative analysis of mRNA expression, cDNA synthesis and qRT-PCR were performed as described above. The PCR reaction was carried out at 50°C for 2 min, 95°C for 10 min, followed by 40 amplification cycles at 95°C for 15 seconds and 60°C for 1 min. GAPDH was used as the internal reference. The sequences of the primers were as follows: CysLT2 receptor forward: 5'-GTC CAC GTG CTG CTC ATA GG-3'; reverse: 5'-ATT GGC TGC AGC CAT GGT C-3'. GAPDH forward: 5'-GTC GGT GTG AAC GGA TTT GG-3'; reverse: 5'-GCT CCT GGA AGA TGG TGA TGG-3'.

Western blot analysis

Electrophoresis and the following Western blot analysis are indispensable to investigate protein changes in the microglia and mouse cerebrum. The homogenates were centrifuged at 10,000 × g at 4°C for 10 min to remove debris. Proteins (30 μg) of the supernatant were determined using protein assay kits (Bio-Rad, Hercules, CA, USA) with bovine serum albumin (Sigma-Aldrich Corporation, St. Louis, MO, USA) as standard. Proteins were diluted 1:1 in loading buffer (10% sodium dodecyl sulphate (SDS), 2% glycerol,

5% bromophenol blue, 2-mercaptoethanol and 0.5 M Tris-HCl; pH 6.8). The mixture samples were boiled for 5 min before being subjected to 10% SDS-polyacrylamide gel electrophoresis (SDS-PAGE) at room temperature and 110 V for 90 min and electrotransferred to polyvinylidene fluoride membranes (PVDF) (Pall Corporation, Coral Gables, FL, USA) at a constant current of 30 V and at 4 ° C overnight. Subsequently, the PVDF membranes were washed twice in phosphate buffered saline (PBS) containing 0.1% Tween 20 (PBS-T) for 10 min at room temperature. This process was carried out three times. The membrane surface was then blocked with 5% fat free dry milk in PBS at 37°C for 1 h and saturated three times with PBS-T for 10 min at room temperature. Subsequently, the membranes were incubated in primary antibodies diluted at 1:1000 at 37°C for 1 h. After three washes with PBS-T, PVDF membranes were incubated with horseradish peroxidase conjugated secondary antibodies diluted at 1:10000 at 37°C for 1 h to detect the bound primary antibody. The labelled proteins were visualised using an enhanced chemiluminescence detection system (Amersham Biosciences, Amersham, UK), and the densities of the specific immunoreactive bands were quantified with a computer-assisted imaging densitometer system.

Flow cytometry

N9 microglial cells were cultured in 12-well plates (Corning) at a concentration of 1×10^5 cells per well. After formation of a monolayer, cells were stimulated with 50 μg/mL of ESPs and treated with 10 μM HAMI3379 for 12 h. Cell surface markers were stained with primary anti-mouse CD80 monoclonal antibody and anti-mouse CD206 monoclonal antibody for 30 min at 4°C. After washing twice with PBS, cells were treated with secondary PE-conjugated goat anti-mouse IgG H&L antibody for 30 min at 4°C and washed twice with PBS. To observe the expression of CD80 and CD206, the cell surface, cells were resuspended in 0.4 mL of PBS and analyzed to express cell surface proteins using a Cytomics FC500 MLP cytometer (Beckman Coulter Inc., Fullerton, CA, USA).

Enzyme-linked immunosorbent assay (ELISA)

Cerebrum and microglia samples were homogenised using a high-speed homogeniser and centrifuged at 5000 × g at 4°C for 10 min, and then, the supernatants were collected. The expression levels of IL-5、IL-10、TGF-β and TNF-α were measured using ELISA kits according to the manufacturer's instructions (R&D Systems, USA). The absorbance was determined by a VersaMax ELISA microplate reader (Molecular Devices, USA) at a wavelength of 492 nm, and the cytokine concentrations (pg/mL) for each sample were calculated by interpolation from a standard curve.

Evaluation of BBB permeability

BBB permeability was evaluated using Evans blue concentrations in the mouse cerebrum as previously described [13]. Mice were injected with 2% (w/v) Evans blue dye 2% (w/v) (5 ml / kg body weight; Sigma, St. Louis, MO, USA) in saline through the tail vein. After 2 h of circulation, mice were anaesthetised and transcardially perfused with saline to remove intravascular dye. The mouse cerebrum was weighed and homogenised in a 50% trichloroacetic acid solution. The homogenates were centrifuged at 12,000 ×g for 10 min and the supernatants were collected. Each supernatant was measured at 620 nm for absorbance to calculate Evans Blue concentrations using a spectrophotometer (Hitachi U3000, Tokyo, Japan).

Gelatin zymography

The procedures were based on zymography using gelatin-containing SDS polyacrylamide gels as previously described [14]. Unboiled protein samples (30 μg) were added to an equal volume of standard loading buffer prior to loading. Mouse CSF samples were loaded at 7.5% (mass/volume) in polyacrylamide gels containing copolymerised substrate gelatin (0.1%) for SDS-PAGE (Sigma-Aldrich Corporation, St. Louis, MO, USA) to measure gelatinase activities. SDS-PAGE was performed in a running buffer (1% SDS, 25 mM Tris, and 250 mM glycine) at room temperature and 110 V for 1 h. After electrophoresis, each gel was washed twice for 30 min in each case in denaturing buffer (2.5% Triton X-100) at room temperature and washed twice with double distilled water at room temperature for 10 min. The gel was then incubated in reaction buffer (50 mM Tris-HCl, pH 7.5; containing 0.01% NaN_3, 0.02% Brij-35 and 10 mM $CaCl_2$) at 37°C for 18 h, stained with 0.25% Coomassie Brilliant Blue R-250 (Bio-Rad, Hercules, CA, USA) for 1 h and destained in a solution of 15% methanol/7.5% acetic acid. The final gel presented a uniform background, except in regions where the gelatinases had migrated and cleaved their respective substrates. Gelatinases were quantitatively analysed using a computer-assisted imaging densitometer system (UN-SCAN-ITTM gel Version 5.1, Silk Scientific, Provo, Utah, USA).

Statistical analysis

Kruskal-Wallis nonparametric analysis followed by Dunn multiple comparison tests was done to evaluate differences among the different groups of mice. All results were presented as means ± standard deviation (SD). Statistical significance was established for P values < 0.05.

Results

Effects of HAMI 3379 on CysLT2R

The qRT-PCR results showed weak expression of the CysLT2 receptor mRNA in uninfected control mice. The expression of CysLT2 receptor mRNA increased significantly increased after *A. cantonensis* infection compared to un-infected mice. CysLT2 receptor mRNA were significantly reduced in mice treated with HAMI3379, albendazole, or or HAMI3379 + albendazole co-therapy. Furthermore, the protein levels of the CysLT2 receptor confirmed the results (Fig. 1).

Effects of HAMI 3379 on eosinophil counts

Eosinophils were identified using the Unopette stained system. Eosinophil counts increased significantly in *A. cantonensis*-infected mice compared to those of uninfected mice. Eosinophils were significantly reduced in mice treated with HAMI3379, albendazole, or HAMI3379 + albendazole co-therapy (Fig. 2).

Effects of HAMI 3379 on brain edema

The water content of the ipsilateral hemisphere and the contralateral hemisphere increased significantly on days 20 after *A. cantonensis* infection compared to the control group. The water content was significantly decreased in mice treated with HAMI3379, albendazole, or HAMI3379 + albendazole compared to infected-untreated mice. No significant differences were detected in the water content in the cerebellum of all groups (Fig. 3).

Changes of M1/M2 polarisation markers when microglia were treated with HAMI3379

The cell surface protein expression of CD80 and CD206 in microglia stimulated with ESPs were significantly higher than the control group. M1-specifc marker CD80 was downregulated in the HAMI3379-treated group. In contrast, cell surface expression of the M2-specifc marker CD206 was significantly upregulated expression. Additionally, the protein assay showed that iNOS, IL-5, TNF-α, Arg-1, IL-10, and TGF-β in the ESPs-stimulated microglia were significantly higher than those of the control group. In the treatment groups with HAMI3379, protein levels of iNOS, IL-5, TNF-α, and Arg-1 were markedly lower ($P < 0.05$) than in the group stimulated with ESPs. However, the protein levels of IL-10, and TGF-β were markedly higher ($P < 0.05$) than in the ESPs-stimulated microglia group (Fig. 4).

Changes of M1/M2 polarisation markers when mice were treated with HAMI3379

The protein levels of CD80, CD206, iNOS, IL-5, TNF-α, Arg-1, IL-10, and TGF-β in mice infected with *A. cantonensis* were significantly higher than those in the control group. In the treatment groups with HAMI3379, albendazole or HAMI3379 + albendazole, the protein levels of CD80, iNOS, Arg-1, IL-5 and TNF-α protein levels were markedly lower ($P < 0.05$) than in the group infected with *A. cantonensis.* However, the protein levels of CD206, IL-10, and TGF-β were markedly higher ($P < 0.05$) than in the group of *A. cantonensis*-infected mice (Fig. 5)

Effects of HAMI3379 on BBB permeability

The disruption of the BBB was estimated through Evans blue extravasation in the mouse model. Evans blue concentration is an indicator of BBB leakage during *A. cantonensis* infection in mice. BBB permeability increased significantly in mice infected with *A. cantonensis* compared to that in the uninfected mice. However, BBB permeability was significantly attenuated in mice treated with HAMI3379 alone, albendazole alone, or HAMI3379 + albendazole cotreatment (Fig. 6).

Effects of HAMI3379 on MMP-9 activity and microRNA-155

Gelatin zymography measures showed that MMP-9 activity increased significantly ($P < 0.05$) in *Mice infected with A. cantonensis*-infected mice compared to uninfected control mice. *A. cantonensis* that received HAMI3379 alone, albendazole alone or HAMI3379 + albendazole cotreatment showed

significantly reduced ($P < 0.05$) MMP-9 activity. MicroRNA-155 showed up-regulation in *A. cantonensis*-infected mice compared to the negative control. MicroRNA-155 was 15 times higher in eosinophilic meningoencephalitis and 20 times higher after HAMI3379 treatment. However, albendazole or HAMI3379 + albendazole cotreatment showed a down-regulation relative to positive control (Fig. 7).

Effects of HAMI3379 on the BBB-related protein

The Western blot assay showed that protein levels of S100B, GFAP, fibronectin, and claudin-5 in the group infected with *A. cantonensis* were significantly higher than in the control group. In the treatment groups with HAMI3379, albendazole, or HAMI3379 + albendazole co-therapy, the protein levels of S100B, GFAP, fibronectin, and claudin-5 were markedly lower ($P < 0.05$) than those of the group infected with *A. cantonensis* (Fig. 8).

Discussion

Cysteinyl leukotrienes modulate inflammatory responses through their receptors, CysLT1R and CysLT2R. In the CNS, the CysLT1 receptor regulates increased BBB permeability and related vasogenic brain edema, astrocyte proliferation, and inflammatory responses after brain ischemia [9]. However, the pathophysiological roles of CysLT2R are less well known in the CNS. Therefore, the present study was designed to investigate the role of the CysLT2 receptor in *A. cantonensis*-induced eosinophilic meningoencephalitis and related mechanisms in mice. Our results showed that both the CysLT2 receptor expression of the mRNA and the protein level were up-regulated in mouse brains were upregulated in the *A. cantonensis* and reduced by HAMI3379. These results were similar to infiltrated eosinophils. The increased expressions were related to eosinophil counts and eosinophils were significantly reduced in mice treated with HAMI3379. These results suggest that CysLT2 receptors may be involved in *A. cantonensis*-induced eosinophilic meningoencephalitis.

An inflammatory response that may have a significant impact on the formation of brain edema. A critical event in the development of brain edema is the breakdown of the BBB, which may be initiated and regulated by several pro-inflammatory mediators (oxidative mediators, adhesion molecules, cytokines, chemokines). These mediators not only regulate the magnitude of leukocyte extravasation into brain parenchyma, but also act directly on brain endothelial cells, causing loosening of junction complexes between endothelial cells, increasing the permeability of the brain endothelial barrier, and causing vasogenic edema [3]. In this study, we found that HAMI3379 significantly decreased BBB dysfunction and pro-inflammatory mediators (CD80, iNOS, IL-5 and TNF-α). Furthermore, measurements of brain water content revealed that *A. cantonensis* infection increased cerebral edema in the ipsilateral and contralateral hemispheres without affecting the cerebellum. Decreased brain edema was present in mice treated with HAMI3379. These results suggest that HAMI3379 inhibits the degree of brain edema in angiostrongyliasis meningoencephalitis.

CysLT2R is a potent receptor for inflammatory mediators, but the mechanism by CysLT2R that regulates angiostrongyliasis meningoencephalitis remains unclear. Microglia activation plays an important role in

regulating inflammatory and immune reaction during angiostrongyliasis meningoencephalitis in mice and exerts pro-inflammatory or anti-inflammatory effect depending on the polarization phenotype [15]. The anti-inflammatory molecules expressed by microglia (e.g., IL-10, IL-4, IL-13, and TGF-β) can limit the recruitment of neutrophils and other lymphocytes to the injury area and decrease leakage of the BBB [16]. Here, we found that HAMI3379 significantly decreased protein levels of M1 polarisation markers (CD80, iNOS, IL-5 and TNF-α), increased the expression of M2 polarisation markers (CD206, IL-10 and TGF-β) both *in vivo* and *in vitro*. These findings indicate that CysLT2R was involved in brain inflammation by inducing the activation of microglia M1 polarisation, inhibiting microglia M1 polarisation, and promoting microglia polarisation towards the M2 phenotype, which can exert neuroprotective effects, and targeting CysLT2R may be a new therapeutic strategy against angiostrongyliasis meningoencephalitis.

Microglia Arg1 are involved in the prevention of NO production, which arginases can compete with NO synthases for their common substrate, arginine [17]. NO is believed to be involved in directly killing pathogens, successful chronic infections are associated with pathogen-induced Arg1 expression, which in turn keeps NO production in check. However, it remains uncertain whether any of these or other potentially associated mechanisms are important in regulating the microglia-mediated killing of *A. cantonensis*. We use HAMI3379 to antagonize CysLT2R and find that only a trend in M2 polarisation marker Arg-1 decreased after HAMI3379 treatment both *in vitro* and *in vivo*. Reduction of arg-1 can increase the bioavailability of arginine by nitric oxide synthase through competition for the arginine substrate, thus increasing NO production and thereby increasing the resistance to parasites. In fact, the decrease in Arg1 was associated with increased microglial NO production and was associated with better control of *A. cantonensis*. It could be due to a potent resistance mechanism to *A. cantonensis* infection.

MMP-9 could cause disruption of the BBB and promote eosinophil infiltration into the cerebral parenchyma via BBB leakage during infection with *A. cantonensis.* This enzyme could cause claudin-5 degradation at the tight junction, collagen type IV degradation in the basal membranes, and increased S100B in astrocytes from wild-type mice. Furthermore [18]. In this study, MMP-9 decreased significantly after HAMI3379 compared with *A. cantonensis* mice. These results suggest that MMP-9 plays a role in the damaged BBB structure and mediating the infiltration of eosinophils into the brain during meningoencephalitis caused by *A. cantonensis*. Brain endothelial microRNA-155 negatively regulates BBB function, making it a novel therapeutic target for neuroinflammatory disorders associated with BBB breakdown [19]. MicroRNA miR-155-5p knockdown attenuates *A. cantonensis*-induced eosinophilic meningitis by downregulating MMP9 and TSLP proteins [20]. We have identified microRNA-155 as a critical microRNA in eosinophilic meningoencephalitis in the BBB. MicroRNA-155 was 15 times higher in eosinophilic meningoencephalitis and 20 times higher after HAMI3379 treatment. In contrast, albendazole treatment showed a down-regulation relative to positive control. The possible reason was that the larvae of *A. cantonensis* in the brains of mice were almost eliminated by albendazole and cannot cause BBB dysfunction. These results suggested that microRNA-155 is a negative regulator of BBB function that may constitute a novel therapeutic target for eosinophilic meningoencephalitis.

BBB disruption is associated with tight junctionprotein degradation, basal membrane disruption, and astrocyte damage after *A. cantonensis* infection. [18]. Vessel-associated microglia maintain BBB integrity through the production of the tight junction protein claudin-5 and physical communication with endothelial cells [21]. In this study, HAMI3379 decreased the permeability of the BBB and down-regulated the expressions of claudin-5. The results showed that the blocking of CysLT2R, along with the changes in claudin-5, may be closely related to BBB damage and meningoencephalitis changes in HAMI3379 treated mice. Additionally, the BBB-related proteins including S100B, GFAP, and fibronectin were markedly lower after HAMI3379 treatment than those of the group infected with *A. cantonensis*. These results related to the reduction of infiltrated eosinophils in angiostrongyliasis meningoencephalitis. These may be due to the effect of the CysLT2R antagonist HAMI3379 on decreasing the damage to the BBB. Inhibition of BBB dysfunction by blocking CysLT2R may have a profound effect on the reduction of brain edema and eosinophilic meningoencephalitis.

We proposed a possible mechanism (Fig. 9) to explain the neuroprotective effects of the CysLT2R antagonist on *A. cantonensis*-induced eosinophilic meningoencephalitis in mice. M1 polarisation markers treated with HAMI3379 decreased significantly; however, the M2 polarisation markers increased. *A. cantonensis* infection disrupts the structure of the BBB and leads to migration of eosinophils across the BBB during *A. cantonensis* infection. This infection induced the activation of inflammatory factors and infiltration of eosinophils. HAMI3379 attenuates the damage from the BBB and inhibits the inflammatory reaction after *A. cantonensis* infection. Our results demonstrated that the selective CysLT2R antagonist HAMI3379 has neuroprotective effects on *A. cantonensis*-induced eosinophilic meningoencephalitis.

Conclusion

The present study is the first to investigate the potential of HAMI3379 for the treatment of brain edema and eosinophilic meningoencephalitis. The promising effect of HAMI3379 in improving *A. cantonensis*-induced brain edema and eosinophilic meningoencephalitis may present a considerable clinical advantage for angiostrongyliasis meningoencephalitis therapy.

Abbreviations

BBB: blood–brain barrier; CysLTs: Cysteinyl leukotrienes; ELISA: Enzyme-linked immunosorbent assay; ESPs: excretory and secretory products; iNOS: inducible nitric oxide synthase**;** IL-5: Interleukin-5; IL-10: Interleukin-10; MMP-9: matrix metalloproteinase-9; qRT-PCR: Quantitative reverse transcription-PCR; TGF-β: Transforming growth factor-β

Declarations

Authors’ contributions

KMC conceived and designed the experiments. SCL wrote the manuscript.

Acknowledgements

The authors wish to thank Ping-Sung Chiu of the Department of Parasitology of Chung Shan Medical University for providing invaluable assistance in the conduct of this study.

Funding

This work was supported by grants from the Chung-Shan Medical University (CSMU-INT-112-18), Taiwan.

Competing interests

The authors declare that they have no competing interests.

Availability of data and materials

Data supporting the conclusions of this article are included within the article and its additional files. The datasets used in the present study are available from the corresponding author upon reasonable request.

Ethics approval and consent to participate

Not applicable.

Consent for publication

Not applicable.

Author details

[1] *Department of Parasitology, Chung Shan Medical University, Taichung 402, Taiwan*

[2] *Clinical Laboratory, Chung Shan Medical University Hospital, Taichung 402, Taiwan*

References

1. Hsu WY, Chen JY, Chien CT, Chi CS, Han NT. Eosinophilic meningitis caused by *Angiostrongylus cantonensis*. Pediatr. Infect. Dis. J. 1990; 9:443–445. doi: 10.1097/00006454-199006000-00016.
2. OuYang L, Wei J, Wu Z, Zeng X, Li Y, Jia Y, Ma Y, Zhan M, Lei W. Differences of larval development and pathological changes in permissive and nonpermissive rodent hosts for *Angiostrongylus cantonensis* infection. Parasitol. Res. 2012; 111:1547–1557. doi: 10.1007/s00436-012-2995-6.
3. Stamatovic SM, Dimitrijevic OB, Keep RF, Andjelkovic AV. Inflammation and brain edema: new insights into the role of chemokines and their receptors. Acta Neurochir Suppl. 2006; 96:444–450. doi: 10.1007/3-211-30714-1_91.

4. Mracsko E, Veltkamp R. Neuroinflammation after intracerebral hemorrhage. Front Cell Neurosci. 2014; 8:388. doi: 10.3389/fncel.2014.00388.
5. Muoio V, Persson PB, Sendeski MM. The neurovascular unit - concept review. Acta Physiol (Oxf). 2014; 210:790–798. doi: 10.1111/apha.12250.
6. Morrison HW, Filosa JA. Stroke and the neurovascular unit: glial cells, sex differences, and hypertension. Am. J. Physiol. Cell Physiol. 2019; 316:C325-C339. doi: 10.1152/ajpcell.00333.2018.
7. Liu LR, Liu JC, Bao JS, Bai QQ, Wang GQ. Interaction of Microglia and Astrocytes in the Neurovascular Unit. Front Immunol. 2020; 11:1024. doi: 10.3389/fimmu.2020.01024.
8. Kanaoka Y, Boyce JA. Cysteinyl leukotrienes and their receptors: cellular distribution and function in immune and inflammatory responses. J. Immunol. 2004; 173:1503–1510. doi: 10.4049/jimmunol.173.3.1503.
9. Zhang LH, Zho JB, Wang YF. Research advance in cysteinyl leukotriene receptors with brain injury. Zhejiang Da Xue Xue Bao Yi Xue Ban 2008; 37:315 – 20. doi: 10.3785/j.issn.1008-9292.2008.03.018.
10. Chiu PS, Lai SC. Matrix metalloproteinase-9 leads to claudin-5 degradation via the NF-κB pathway in BALB/c mice with eosinophilic meningoencephalitis caused by *Angiostrongylus cantonensis*. PLoS One. 2013; 8:e53370. doi: 10.1371/journal.pone.0053370.
11. Chen KM, Lan KP, Lai SC. Heme oxygenase-1 modulates brain inflammation and apoptosis in mice with angiostrongyliasis. Parasitol. Int. 2022; 87:102528. doi: 10.1016/j.parint.2021.102528.
12. Wei S, Sun J, Li J, Wang L, Hall CL, Dix TA, Mohamad O, Wei L, Yu SP. Acute and delayed protective effects of pharmacologically induced hypothermia in an intracerebral hemorrhage stroke model of mice. Neuroscience 2013; 252:489–500. doi: 10.1016/j.neuroscience.2013.07.052.
13. Chen AC, Shyu LY, Lin YC, Chen KM, Lai SC. Proteasome serves as pivotal regulator in *Angiostrongylus cantonensis*-induced eosinophilic meningoencephalitis. PLoS One. 2019; 14:e0220503. doi: 10.1371/journal.pone.0220503.
14. Chen AC, Shyu LY, Hsin YL, Chen KM, Lai SC. Resveratrol relieves *Angiostrongylus cantonensis*-induced meningoencephalitis by activating sirtuin-1. Acta Trop. 2017; 173:76–84. doi: 10.1016/j.actatropica.2017.05.023.
15. Wei J, Wu F, He A, Zeng X, Ouyang LS, Liu MS, Zheng HQ, Lei WL, Wu ZD, Lv ZY. Microglia activation: one of the checkpoints in the CNS inflammation caused by *Angiostrongylus cantonensis* infection in rodent model. Parasitol. Res. 2015; 114:3247–3254. doi: 10.1007/s00436-015-4541-9.
16. Kang R, Gamdzyk M, Lenahan C, Tang J, Tan S, Zhang JH. The Dual Role of Microglia in Blood-Brain Barrier Dysfunction after Stroke. Curr. Neuropharmacol. 2020; 18:1237–1249. doi: 10.2174/1570159X18666200529150907.
17. Sawano T, Tsuchihashi R, Watanabe F, Niimi K, Yamaguchi W, Yamaguchi N, Furuyama T, Tanaka H, Matsuyama T, Inagaki S. Changes in L-arginine metabolism by Sema4D deficiency induce promotion of microglial proliferation in ischemic cortex. Neuroscience 2019; 406:420–431. doi: 10.1016/j.neuroscience.2019.03.037.

18. Chiu PS, Lai SC. Matrix metalloproteinase-9 leads to blood-brain barrier leakage in mice with eosinophilic meningoencephalitis caused by *Angiostrongylus cantonensis*. Acta Trop. 2014; 140:141–150. doi: 10.1016/j.actatropica.2014.08.015.
19. Lopez-Ramirez MA, Wu D, Pryce G, Simpson JE, Reijerkerk A, King-Robson J, Kay O, de Vries HE, Hirst MC, Sharrack B, Baker D, Male DK, Michael GJ, Romero IA. MicroRNA-155 negatively affects blood-brain barrier function during neuroinflammation. FASEB J. 2014; 28:2551–2565. doi: 10.1096/fj.13-248880.
20. Zhou X, Zhang J, Liu J, Guo J, Wei Y, Li J, He P, Lan T, Peng L, Li H. MicroRNA miR-155-5p knockdown attenuates *Angiostrongylus cantonensis*-induced eosinophilic meningitis by downregulating MMP9 and TSLP proteins. Int J Parasitol. 2021; 51:13–22. doi: 10.1016/j.ijpara.2020.07.013.
21. Haruwaka K, Ikegami A, Tachibana Y, Ohno N, Konishi H, Hashimoto A, Matsumoto M, Kato D, Ono R, Kiyama H, Moorhouse AJ, Nabekura J, Wake H. Dual microglia effects on blood brain barrier permeability induced by systemic inflammation. Nat. Commun. 2019; 10:5816. doi: 10.1038/s41467-019-13812-z.

Figures

Figure 1

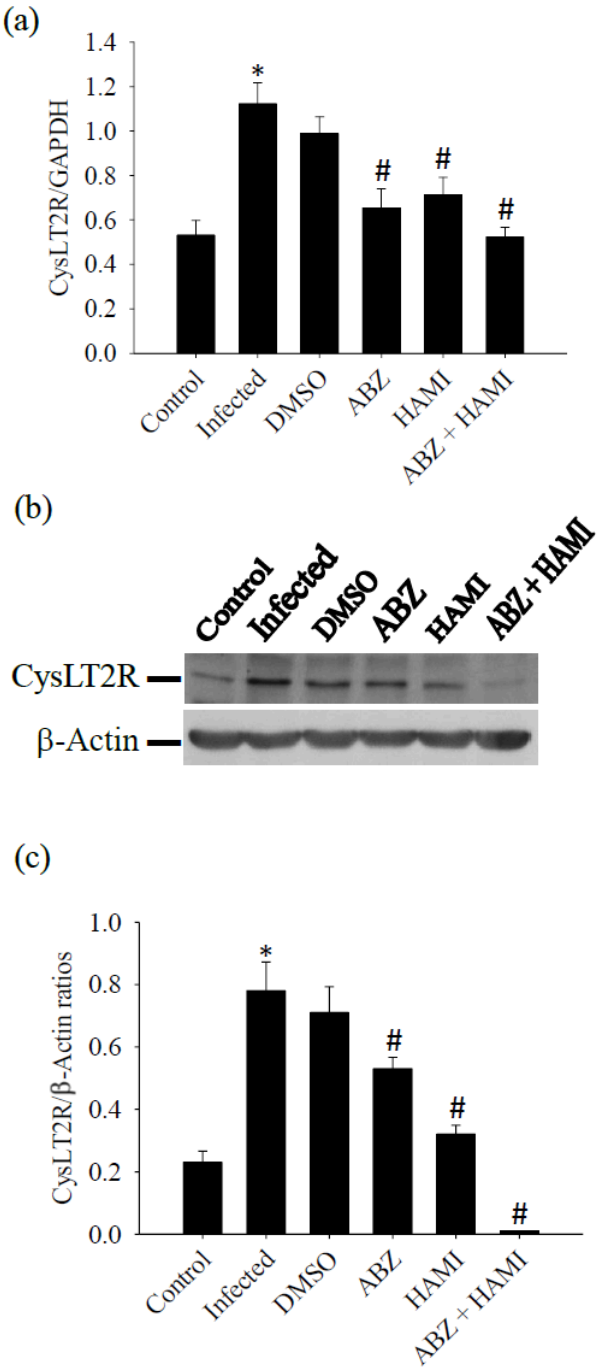

Figure 1

Effects of HAMI3379 on cysteinyl leukotriene 2 receptor (CysLT2R). (a) Expression level of CysLT2R mRNA in mice cerebrum. The relative levels of mRNA were estimated by normalizing the expression to that of GADPH. (b) Cerebrum protein levels were analysed by immunoblotting for CysLT2R. β-Actin was used as a loading control. (c) CysLT2R quantification and normalisation were performed with a computer-assisted imaging densitometer system. * indicates a statistically significant increase in mice

infected with *Angiostrongylus cantonensis* compared to the control. [#]indicates a statistically significant decrease in treated mice compared to infected mice with *A. cantonensis.*

Figure 2

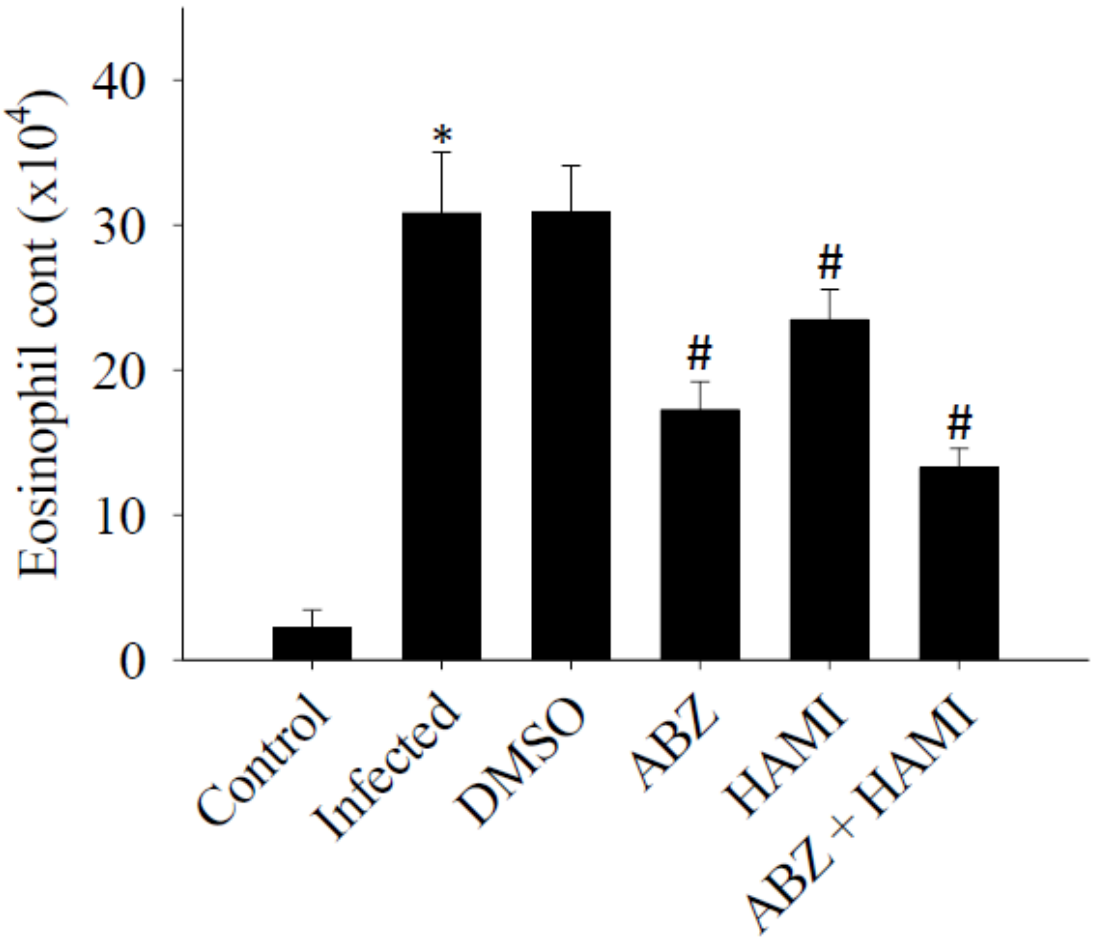

Figure 2

Effects of HAMI3379 on eosinophil counts. Eosinophil counts increased significantly increased (*P < 0.05) in *Angiostrongylus cantonensis*-infected mice compared to non-infected controls. Treatment with HAMI3379 alone, albendazole alone, or albendazole + HAMI3379 co-therapy significantly decreased ([#]P < 0.05) the levels compared to infected mice.

Figure 3

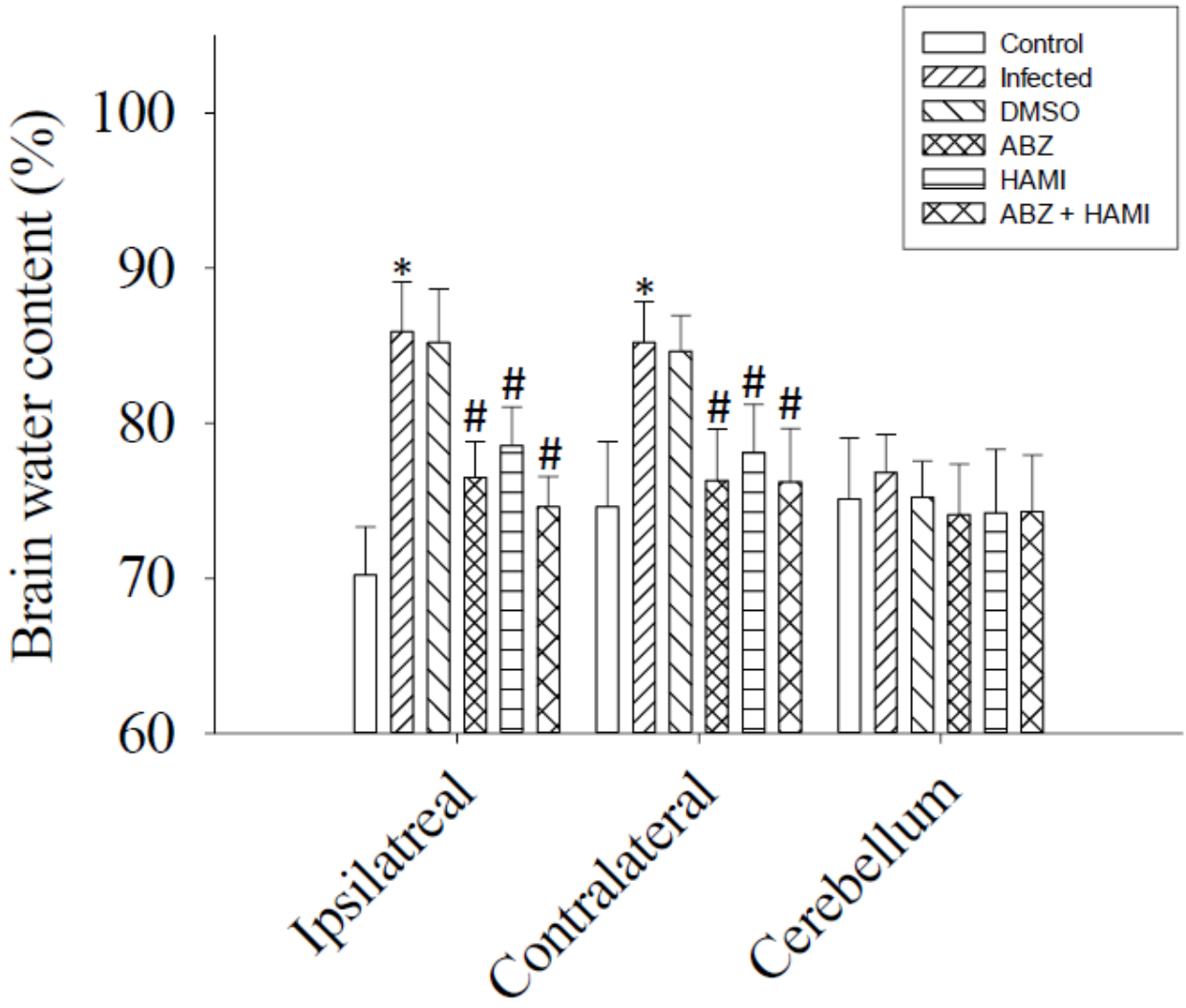

Figure 3

Effects of HAMI3379 on brain edema. Water content in the ipsilateral hemisphere, contralateral hemisphere and cerebellum. n=3 mice per group. *Angiostrongylus cantonensis*-infected mice were treated with DMSO, albendazole, HAMI3379 or albendazole+HAMI3379 co-therapy. *indicates a statistically significant increase in mice infected to *A. cantonensis* compared with the control. #indicates a statistically significant decrease in treated mice compared to infected mice with *A. cantonensis.*

Figure 4

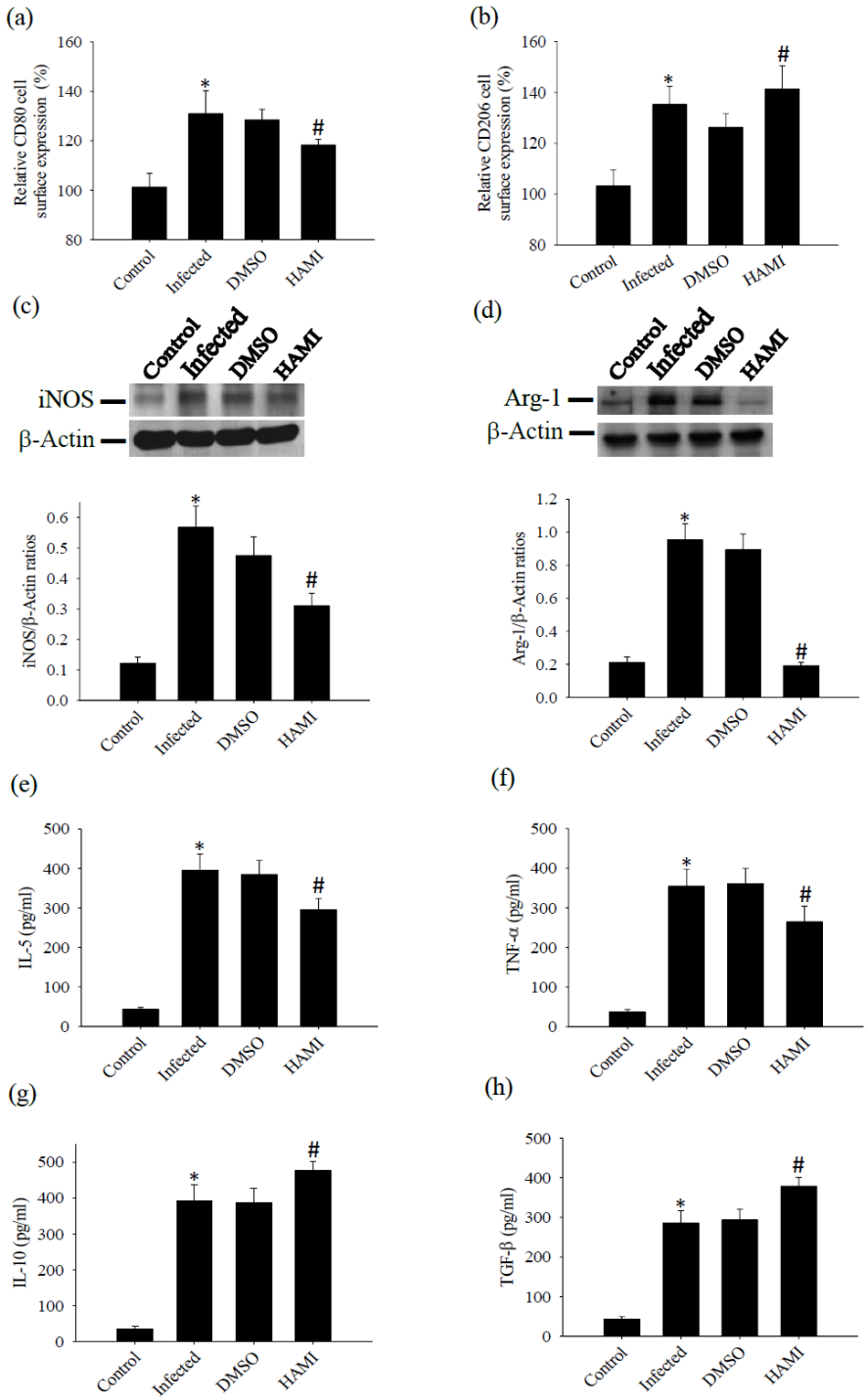

Figure 4

Changes of M1/M2 polarisation markers when microglia were treated with HAMI3379. Relative cell surface protein expression of the M1-specified marker CD80 (a) and the M2-specified marker CD206 (b) was determined by Flow cytometry. Western blot was used to detect protein levels of iNOS (c) and Arg-1 (d). β-Actin was used as a loading control. Protein levels of iNOS and Arg-1 were quantified using a computer-assisted imaging densitometer system. The productions of IL-5 (e), TNF-α (f), IL-10 (g), and

TGF-β (h) in the microglia were tested using ELISA kits. Microglia stimulated with ESPs were treated with DMSO or HAMI3379. * indicates a statistically significant increase in the ESPs-stimulated microglia compared to the control. # indicates a statistically significant change in the treated microglia compared to the ESPs-stimulated microglia.

Figure 5

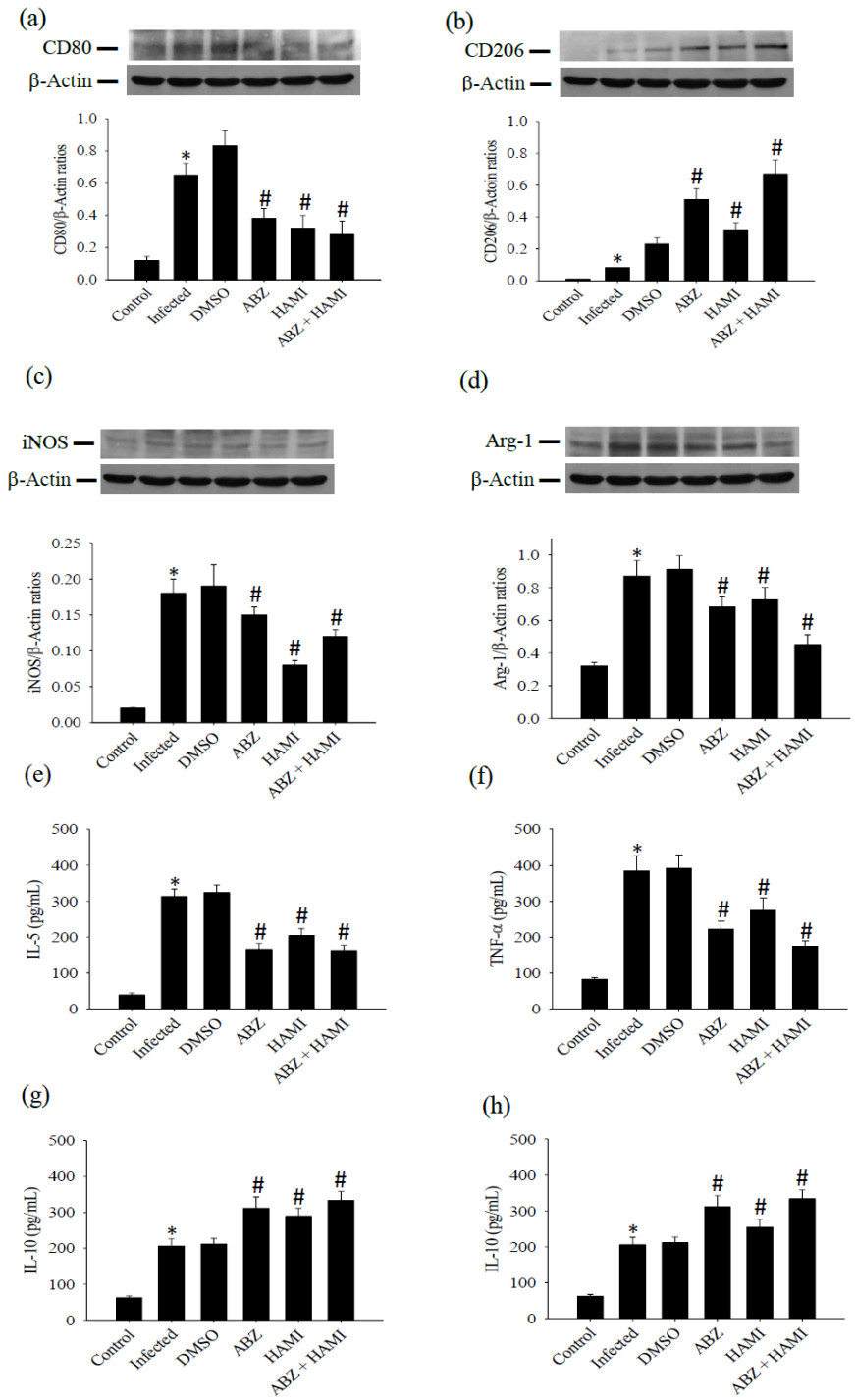

Figure 5

Changes of M1/M2 polarisation markers when mice were treated with HAMI3379. Western blot was used to detect protein levels of CD80 (a), CD206 (b), iNOS (c), and Arg-1 (d) from cerebrum. β-Actin was used as a loading control. The protein levels of CD80, CD206, iNOS and Arg-1 were quantified using a computer-assisted imaging densitometer system. Productions of IL-5 (e), TNF-α (f), IL-10 (g), and TGF-β (h) in the cerebrum of mice were tested using ELISA kits. Mice infected with *Angiostrongylus cantonensis* were treated with DMSO, albendazole, HAMI3379 or HAMI3379+albendazole co-therapy. * Indicates a statistically significant increase in *A. cantonensis*-infected mice compared to the control. # indicates a statistically significant change in treated mice compared to the *A. cantonensis*-infected mice.

Figure 6

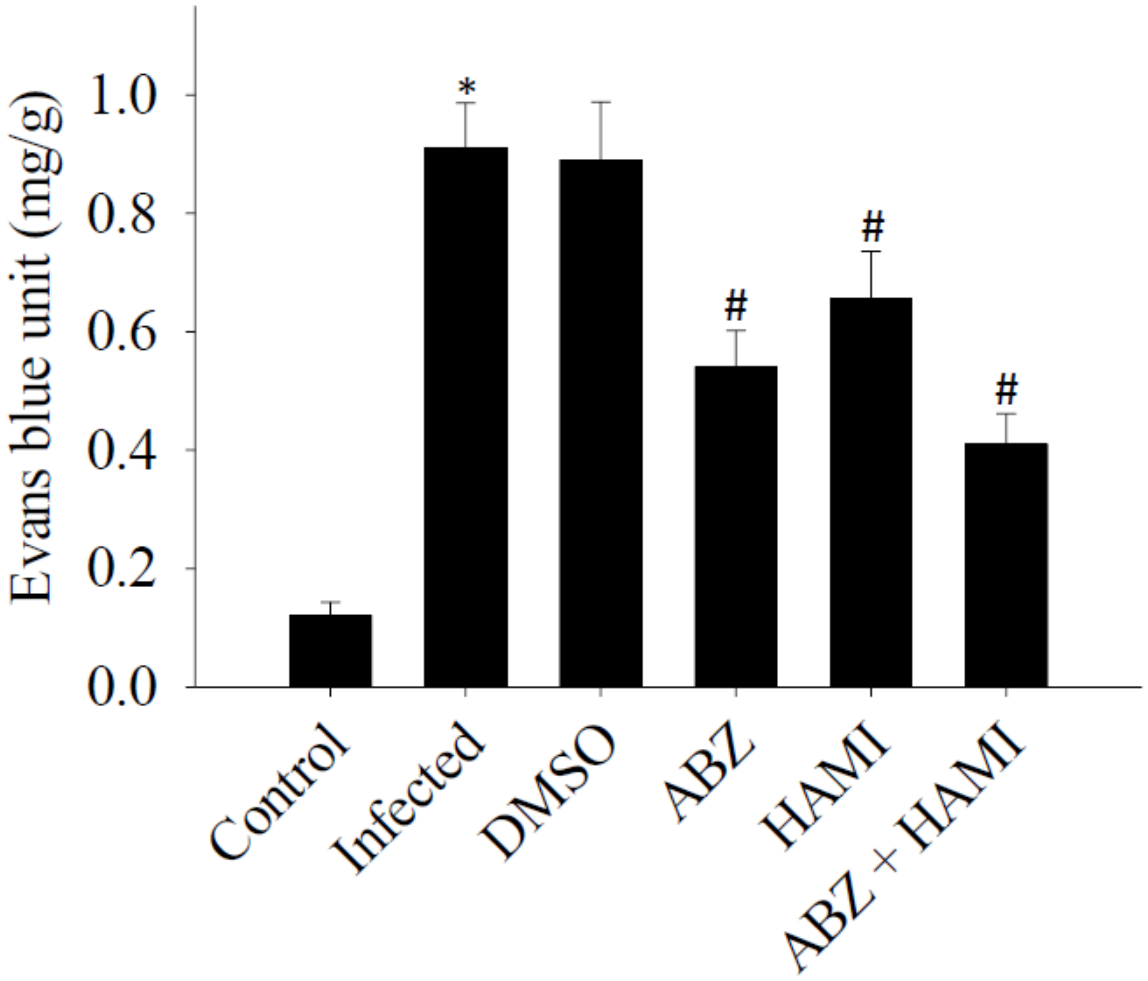

Figure 6

Effects of HAMI3379 on the permeability of the blood-brain barrier (BBB). Evans Blue detected mouse BBB permeability during *Angiostrongylus cantonensis* infection. Evans blue dye units increased significantly (*$P < 0.05$) in *A. cantonensis*-infected mice (infected) compared to uninfected controls. Mice treated with HAMI3379, albendazole, or HAMI3379+albendazole showed significantly lower ($^{\#}P < 0.05$) Evans Blue dye units compared to untreated mice infected with *A. cantonensis*.

Figure 7

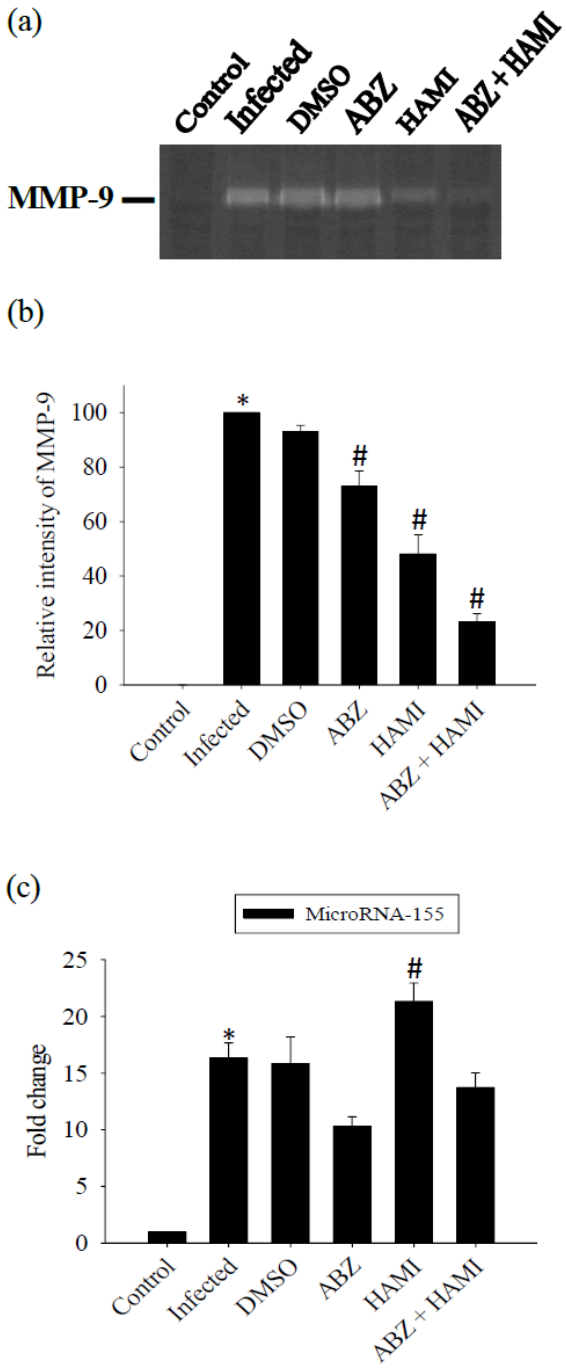

Figure 7

Effects of HAMI3379 on matrix metalloproteinase-9 (MMP-9) and microRNA-155. (a) Enzyme intensities were analysed by zymography for MMP-9 from the cerebrospinal fluid. Mice infected with *Angiostrongylus cantonensis* were treated with DMSO, HAMI3379, albendazole, or HAMI3379+albendazole co-therapy. (b) Quantification of MMP-9 was performed with a computer-assisted imaging densitometer system. (c) The expression levels of cerebrum microRNA-155 was estimated by normalizing the expression to that of U6. * indicates a statistically significant increase in mice infected with *A. cantonensis* compared to the control. # indicates a statistically significant increase in treated mice compared to infected mice with *A. cantonensis.*

Figure 8

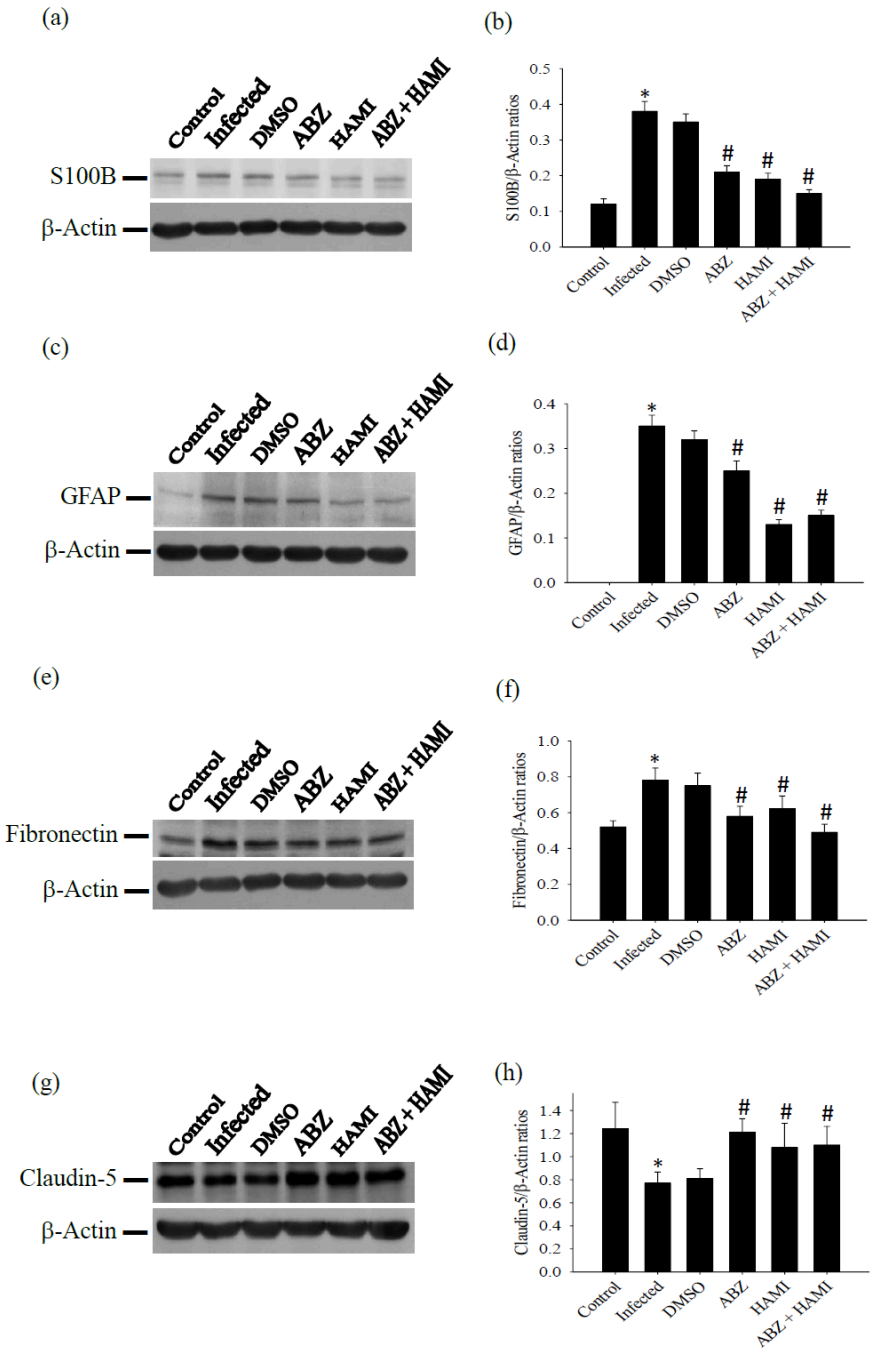

Figure 8

Effects of HAMI3379 on proteins related to the blood-brain barrier. Cerebrum protein levels were analysed by Western blotting for S100B (a), GFAP (c), fibronectin (e), and claudin-5 (g). Infected mice were treated with albendazole, HAMI3379, or HAMI3379+albendazole co-therapy. β-Actin was used as a loading control. Quantification and normalisation of S100B (b), GFAP (d), fibronectin (f), and claudin-5 (h) were performed with a computer-assisted imaging densitometer system. *indicates a statistically

significant increase in mice infected with *Angiostrongylus cantonensis* compared to the control. # indicates a statistically significant decrease in treated mice compared to infected mice with *A. cantonensis.*

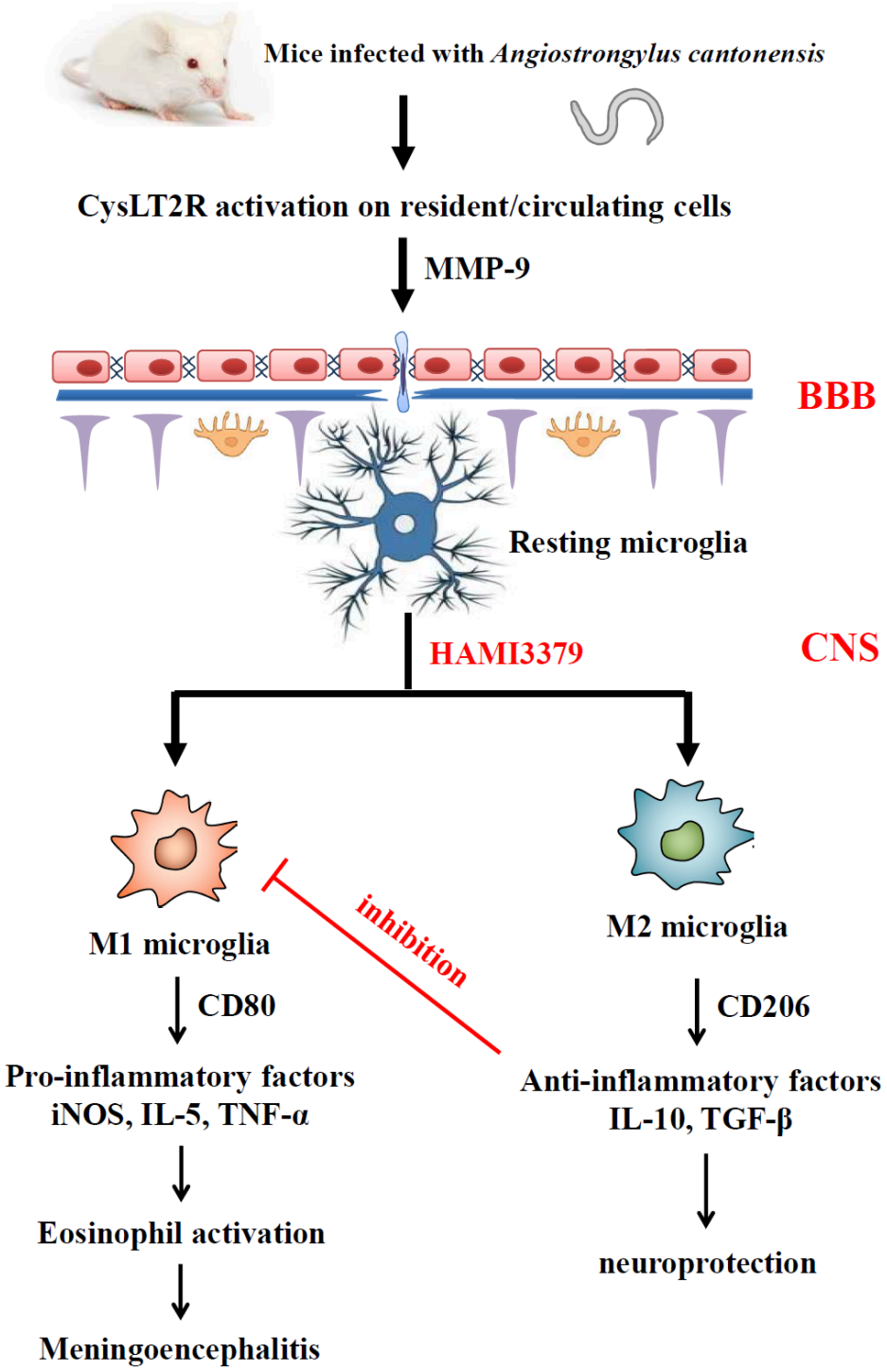

Figure 9

Possible neuroprotective mechanisms of CysLT2R antagonist on *Angiostrongylus cantonensis*-induced edema and eosinophilic meningoencephalitis. Mice infected with *A. cantonensis* that disrupts the

structure of the blood-brain barrier (BBB) and leads to eosinophils migration across the BBB. *A. cantonensis* infection induced the activation of pro-inflammatory factors and eosinophil infiltration. HAMI3379 significantly decreased M1 polarisation markers (CD80, iNOS, IL-5, and TNF-α), increased the expression of M2 polarisation markers (CD206, IL-10 and TGF-β). These results demonstrated that HAMI3379 attenuates BBB damage and inhibits the inflammatory reaction after *A. cantonensis* infection. The selective CysLT2R antagonist HAMI3379 has neuroprotective effects on *A. cantonensis*-induced edema and eosinophilic meningoencephalitis.